Volume 2 | Number 11 | November 2015

Open Access Article. Published on 23 September 2015. Downloaded on 2/11/2026 11:55:22 AM.
This article is licensed under a Creative Commons Attribution 3.0 Unported Licence.

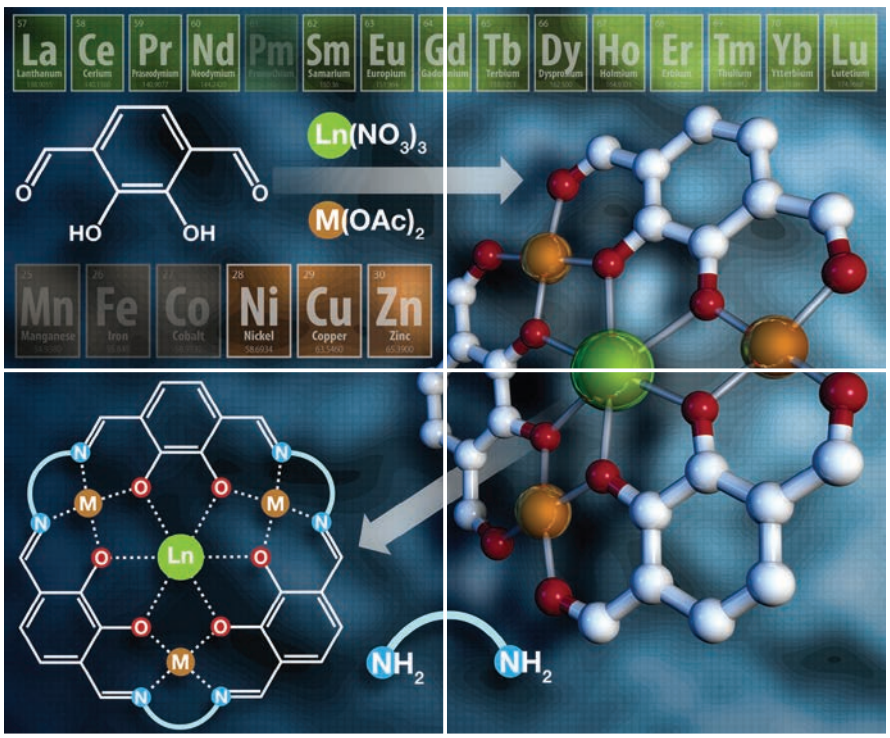

INORGANIC CHEMISTRY

FRONTIERS

Chinese Chemical Society
ROYAL SOCIETY OF CHEMISTRY
http://rsc.li/frontiers-inorganic

View Article Online

INORGANIC CHEMISTRY
FRONTIERS

RESEARCH ARTICLE

CrossMark
click for updates

Cite this: *Inorg. Chem. Front.*, 2015, **2**, 1045

Ultra-rapid microwave synthesis of $Li_{3-x-y}M_xN$ (M = Co, Ni and Cu) nitridometallates†

Nuria Tapia-Ruiz,[a] Josefa Vidal Laveda,[a] Ronald I. Smith,[b] Serena A. Corr[a] and Duncan H. Gregory*[a]

Received 11th August 2015,
Accepted 23rd September 2015

DOI: 10.1039/c5qi00145e

rsc.li/frontiers-inorganic

Single phase nitridometallates $Li_{3-x-y}M_xN$ ($0.05 \leq x \leq 0.27$; M = Co, Ni and Cu) with potential use as negative electrodes in lithium (Li^+) ion batteries have been synthesised in <10 minutes *via* solid state reactions in a single mode cavity microwave reactor without an external susceptor. Reaction times are reduced by up to four orders of magnitude over previous synthetic methods. A combination of powder X-ray and neutron diffraction has provided detailed crystal structures of the vacancy-disordered nitrides. The electrochemical performance of these materials is comparable to that observed in conventionally-heated analogues.

Open Access Article. Published on 23 September 2015. Downloaded on 2/11/2026 11:55:22 AM.
This article is licensed under a Creative Commons Attribution 3.0 Unported Licence.

Introduction

Lithium nitridometallates, $Li_{3-x-y}M_xN$, (M = Co, Ni, Cu) have shown great promise as anodes in Li^+ ion batteries, with competitive capacity and cycleability which is not hampered by significant volume changes on (de)lithiation. For example, $Li_{2.6}Co_{0.4}N$ exhibits a capacity more than twice that of lithiated graphite, at *ca.* 900 mA h g^{-1}.[1] These $Li_{3-x-y}M_xN$ materials have an α-Li_3N-type structure, where the transition metal is incorporated at the interplanar positions (Li(1) sites) and cationic Li^+ vacancies are created in the $[Li_2N]$ planes (Li(2) sites) (Fig. 1).[2] The vacancies provide a mechanism for the exceptionally high ionic conductivity observed in these materials and can be controlled by the transition metal substitution level and the synthesis conditions. Typically, high temperatures and long reaction times are required to make single phase materials (*e.g.* $Li_{3-x-y}Ni_xN$ crystals require heating Li_3N and Ni powders at 853–983 K for 7 days).[3] Ideally sustainable energy materials, such as those employed as electrodes in batteries, should themselves be produced sustainably and energy-efficiently. Reducing processing times and temperatures is an important part of this process and microwave (MW) heating might therefore offer an energy-efficient alternative. MW synthesis of ternary and higher nitrides has so far been limited to five compounds; the anti-fluorites Li_3FeN_2, Li_5TiN_3 and Li_3AlN_2[4] and the nitridosilicates Li_2SiN_2 and $LiSi_2N_3$.[5] The phase purity of the products in these cases was challenging to achieve. Here, we demonstrate that phase-pure α-Li_3N-type ternary nitrides with appreciable vacancy concentrations can be synthesised in minutes using a commercial benchtop MW reactor at 300 W. Furthermore, we compare the electrochemical performance of the materials with their conventionally heated counterparts.

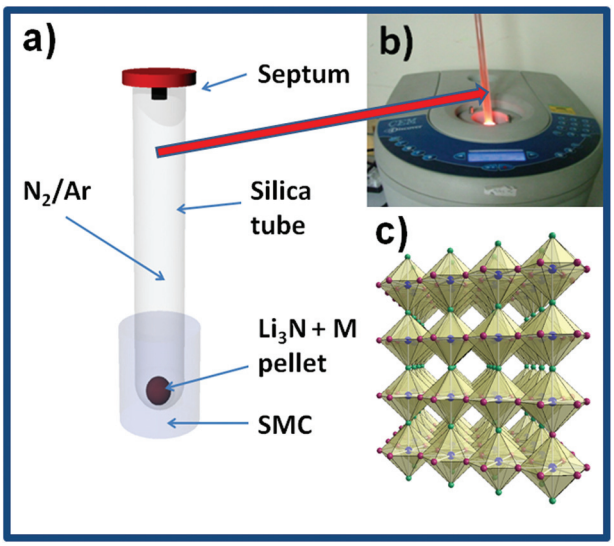

Fig. 1 (a) Schematic experimental configuration for the SMC MW synthesis of lithium nitridometallates; (b) image of reaction in progress; and (c) polyhedral representation of $Li_{3-x-y}M_xN$, where M = Co–Cu. N (blue spheres); Li(2) (pink spheres); and Li(1) (green spheres).

[a]*WestCHEM, School of Chemistry, University of Glasgow, Glasgow G82 5EZ, UK. E-mail: Duncan.Gregory@Glasgow.ac.uk; Fax: +44(0) 1413304888; Tel: +44(0) 1413306438*
[b]*ISIS Facility, Rutherford Appleton Laboratory, Harwell Oxford, Didcot OX11 0QX, UK*

† Electronic supplementary information (ESI) available: Refinement procedures, lattice parameters from XRD, thermal displacement parameters, structure plot, refinement profile plots, schematic and photographs of the synthesis set-up. See DOI: 10.1039/c5qi00145e

Open Access Article. Published on 23 September 2015. Downloaded on 2/11/2026 11:55:22 AM.
This article is licensed under a Creative Commons Attribution 3.0 Unported Licence.

Experimental

Synthesis of $Li_{3-x-y}M_xN$ materials

All manipulations were performed in an N_2-filled glovebox (5 ppm O_2; 10 ppm H_2O). Transition metal powders (Co, Ni, Cu; Laboratory BDH Reagent, 99%) were reduced prior to reaction to remove surface metal oxides (under a flow of H_2/N_2 (95 : 5%) gas at 600 °C for 12 h). Molar ratios of Li_3N powder (Alfa Aesar, 300 mesh, 99.95%; *ca.* 0.1 g) and Co, Ni or Cu metal powder were ground, pressed into pellets (13 mm diameter, 1–2 mm thickness) and placed in a nitrogen-filled silica tube (250 × 8 × 2 mm) sealed with a septum (Fig. 1a). Reactions were conducted in a single mode cavity (SMC) microwave reactor (CEM Discover®, CEM corporation, 300 W max. output, 2.45 GHz) at 300 W to yield black powders (Fig. 1b). Table 1 shows representative experiments performed (**1–7**) and the reaction conditions used for each.

Characterisation

Powder X-ray diffraction (PXD) data from samples **1–7** were collected at room temperature with a PANalytical XPERT Pro MPD diffractometer using a Cu $K\alpha_1$ source. The diffraction data were collected in the range $5 \leq 2\theta \leq 85°$ 2θ with a 0.0168° 2θ step size for 1–12 h, depending on sample quantity and quality. The air sensitive samples were ground into fine powders, which were placed in 0.5 mm diameter sealed glass capillaries for data collection. Experimental diffraction data were compared to powder patterns generated from data in the Inorganic Crystal Structure Database (ICSD)[6] using PowderCell 2.4.[7] X-ray data were indexed and unit cell parameters refined by least squares fitting using the CELREF software package.[8] Crystal structure refinements of compounds **1–7** were performed using time of flight (ToF) powder neutron diffraction (PND) data collected on the POLARIS diffractometer at the UK pulsed spallation neutron source ISIS (Rutherford Appleton Laboratory). For each sample, ~0.1 g of powder were loaded into a thin-walled cylindrical vanadium can and sealed with indium wire in an N_2-filled glovebox. Normalised diffraction patterns from the detector banks centred at $2\theta = 90°$ and $2\theta = 145°$ were used to refine a structural model based on α-Li_3N (in hexagonal space group $P6/mmm$)[2] using the GSAS and EXPGUI software packages.[9,10] Starting lattice parameters were obtained from the PXD data and the initial transition metal occupancy of the interplanar Li(1) site was determined from the reaction stoichiometry.

Galvanostatic measurements at room temperature of samples were conducted over the voltage range of 0–1.4 V at a C/30 rate in a Swagelok-type cell using a BioLogic VSP potentiostat. The working electrode consisted of the active material, $Li_{3-x-y}M_xN$ mixed with carbon black in a weight ratio of 8.5 : 1.5. In each case, the nitride–carbon mixture was mechanically mixed for 15 min using a Retsch MM 200 ball mill in an air-tight, stainless steel sealed container, packed under argon. 0.765 mg active material (**3**) and 1.190 mg active material (**5**) were used in the respective cells. A thin plate of lithium metal (Sigma-Aldrich, 99.9% trace metal basis) was used as a counter electrode. The electrolyte solution used was 1 M $LiPF_6$ dissolved in ethylene carbonate : diethyl carbonate (EC : DEC) in 1 : 1 molar ratio and a Whatman glass filter was used as the separator. Electrode preparation and (dis)assembly of the electrochemical cells were conducted in an Ar-filled glovebox (<0.5 ppm O_2; <0.5 ppm H_2O). Post-cycled electrodes were washed with THF and dried under vacuum for 1 h prior to XRD analysis.

PND structure refinement

In each case, the background was fitted using the reciprocal interpolation function (number 8 within GSAS) employing 10–18 coefficients. The unit cell parameters, peak profile parameters, occupancies of the shared sites (Li(1) and M) and temperature factors were all then refined, followed by the application of an absorption correction. Peak shapes were modelled in each case using ToF profile function 3 (convolution of back-to-back exponentials with a pseudo-Voigt function). At this point, any extra phases such as V from the sample canister (samples **1–7**; see Fig. 3), Li_2O (**5** and **6**) or Li_3N (**7**)) were introduced in the refinement. Lastly, anisotropic temperature factors were refined and the occupancy of the Li(2) site was allowed to vary freely to investigate the possibility of vacancies at this site. Constraints were applied to the fractional occupancies and thermal parameters of the disordered Li(1)/M site such that the total occupancy was unity and the thermal parameters were equal. The refinements were considered complete when convergence was achieved, all the variables were stable and the *R*-values minimised.

Table 1 Summary of reactions (**1–7**), including the experimental parameters and products identified by PXD

Sample	M	Li_3N : M molar ratio	Time (seconds)	Atm.	Products
1	Ni	1 : 0.10	210	N_2	$Li_{3-x-y}Ni_xN$
2	Ni	1 : 0.22	180	N_2	$Li_{3-x-y}Ni_xN$
3	Ni	1 : 0.29	260	N_2	$Li_{3-x-y}Ni_xN$
4	Co	1 : 0.09	60	N_2	$Li_{3-x-y}Co_xN$
5	Co	1 : 0.21	120	N_2	$Li_{3-x-y}Co_xN$, Li_2O
6	Co	1 : 0.30	420 + 420	Ar	$Li_{3-x-y}Co_xN$, Li_2O
7	Cu	1 : 0.11	240	N_2	$Li_{3-x-y}Cu_xN$, Li_3N

Results and discussion

Fig. 2 shows a typical X-ray diffraction pattern of the as-formed products after MW irradiation (for sample **2**). Powder X-ray diffraction data from samples **1–7** revealed phases that were isostructural with α-Li_3N, with reflections shifted in 2θ when compared to the calculated pattern of Li_3N ($P6/mmm$, a = 3.648 (1) Å and c = 3.875(1) Å).[6]

The absence of transition metal reagents in the final PXD patterns of **1–7** indicate full conversion of the initial mixtures to final products (Table 1). The oxidation products of Li_3N or

This journal is © the Partner Organisations 2015

Open Access Article. Published on 23 September 2015. Downloaded on 2/11/2026 11:55:22 AM.
This article is licensed under a Creative Commons Attribution 3.0 Unported Licence.

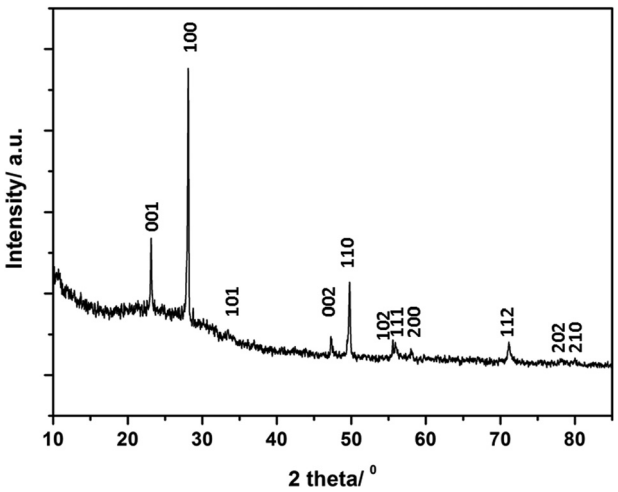

Fig. 2 Typical XRD pattern of a $Li_{3-x-y}M_xN$ sample (M = Co–Cu) synthesised by MW methods (sample **2** is shown). Indices for the expected reflections are indicated.

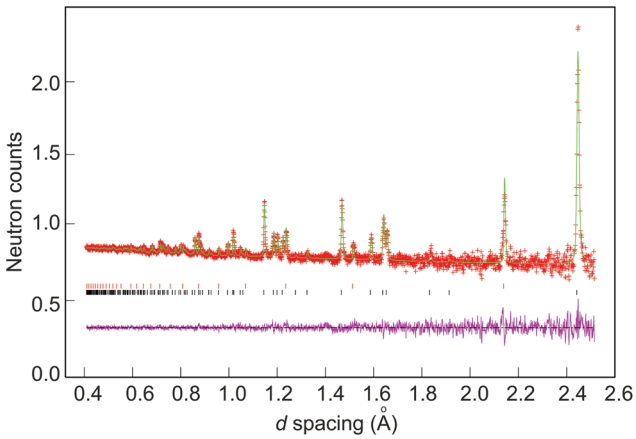

Fig. 3 Rietveld fit against PND data collected at room temperature from sample **4** from the 2θ = 145° (backscattering) detector bank. Observed data points are shown in red, calculated profile in green and the difference (obs–calc) profile in pink. Black and red vertical tick marks indicate reflections from the $Li_{3-x-y}Co_xN$ phase and the vanadium sample can respectively.

Li (Li_2O) found in samples **5** and **6** might originate either from the starting materials and/or air exposure during handling. Lattice parameters of samples (**1–7**) were indexed in the hexagonal space group *P6/mmm* (ESI; Table S1†). Samples **1–6** showed similar trends in cell parameters *vs.* transition metal content to those previously reported by Juza *et al.*;[11] a slight increase in the *a* parameter and a steeper linear decrease in the *c* parameter respectively with increasing metal substitution, *x*. Several authors have observed a similar dependence of the lattice parameters on *x*.[12,13]

Selected room temperature crystallographic information from the MW-synthesised lithium ternary nitrides containing Ni (**1–3**), Co (**4–6**) and Cu (**7**) following Rietveld refinement is shown in Table 2 (with additional information in the ESI†). An example fit to the data is shown in Fig. 3. Despite the small sample volumes used, good fits were obtained and the lattice parameters determined from PND data were in good agreement with those obtained from PXD (ESI; Table S1†). Fig. 4 plots the lattice parameters against the transition metal stoichiometry, *x*, obtained from the refinements against PND data and compares these with those from the literature.[11] For nitridonickelates, our data often reveal larger *c* parameters than those reported previously from PXD data, whereas for nitridocobaltates the sets of data are in very close agreement.[11] The *a* parameter *vs.* *x* relationship closely follows the previously reported trend.

The variations in the *a* and *c* parameters with *x* are directly related to the Li(2)–N and (Li(1)/M)–N distances respectively (Table 2). The reduction in (Li(1)/M)–N bond lengths compared to the equivalent distance in Li_3N (1.9368(1) Å)[2] is attributed to an increase in the covalency of the (Li(1)/M)–N bond due to the presence of the transition metal, which increases the π character of the bond.[14,15]

Table 2 Selected data for samples **1–7** obtained from refinements against ToF PND data from 2θ = 90° and 2θ = 145° banks

Sample	**1**	**2**	**3**	**4**	**5**	**6**	**7**
Stoichiometry	$Li_{2.93}Ni_{0.07}N$	$Li_{2.54}Ni_{0.22}N$	$Li_{2.36}Ni_{0.27}N$	$Li_{2.84}Co_{0.10}N$	$Li_{2.45}Co_{0.17}N$	$Li_{2.41}Co_{0.21}N$	$Li_{2.95}Cu_{0.05}N$
Crystal system	Hexagonal						
Space group	*P6/mmm*						
Z	1						
Density, ρ/g cm^{-3}	1.426	1.673	1.732	1.513	1.559	1.588	1.882
a/Å	3.6675(2)	3.6860(2)	3.6950(2)	3.6679(1)	3.6800(2)	3.6977(2)	3.6675(2)
c/Å	3.8383(4)	3.7700(4)	3.7390(4)	3.8305(2)	3.7931(3)	3.7576(3)	3.7983(2)
V/Å^3	44.712(6)	44.360(6)	44.210(6)	44.629(4)	44.486(5)	44.496(4)	44.245(4)
M occupancy (*x*)	0.069(9)	0.221(2)	0.267(3)	0.102(1)	0.171(2)	0.210(3)	0.051(2)
Li(2) occupancy	1	0.88(4)	0.82(4)	0.97(3)	0.811(4)	0.81(2)	1
(Li(1)/M)–N/ Å	1.9190(2)	1.8850(2)	1.8697(2)	1.9152(1)	1.8965(2)	1.8788(1)	1.9053(2)
Li(2)–N/Å	2.1176(1)	2.1282(1)	2.13360(9)	2.11776(8)	2.1244(1)	2.13499(9)	2.11532(9)
Observations	7261	7364	7428	7728	7326	6949	7670
Parameters	57	49	61	56	59	46	56
R_{wp}	0.0136	0.0181	0.0175	0.0147	0.0126	0.0186	0.0136
R_p	0.0245	0.0313	0.0302	0.0323	0.0192	0.328	0.0293

Open Access Article. Published on 23 September 2015. Downloaded on 2/11/2026 11:55:22 AM.
This article is licensed under a Creative Commons Attribution 3.0 Unported Licence.

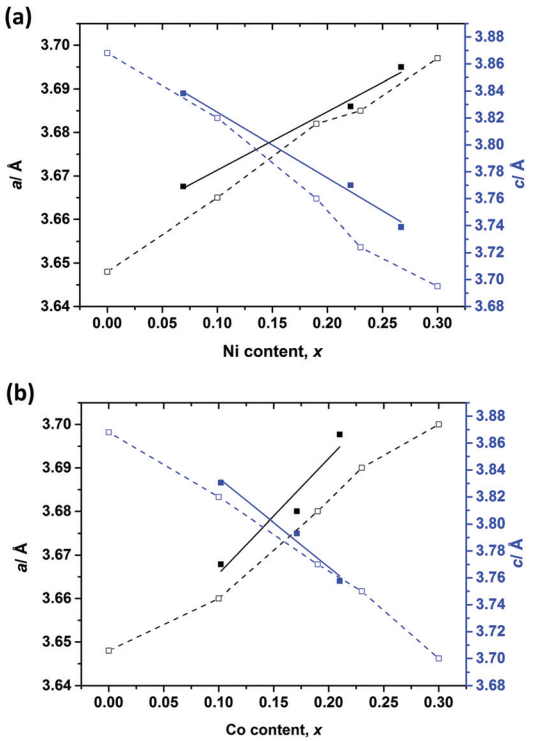

Fig. 4 Variations of unit cell parameters with varying (a) Ni (**1–3**) and (b) Co (**4–6**) substitution levels (x). Filled squares show refined values from our PND data. Empty squares show data from ref. 11. Trend lines serve as a guide to the eye.

Moreover, a slight increase in the interplanar Li(2)–N bond length as the level of dopant increases was also observed. The a parameter (and Li(2)–N distance) has been directly related to the existence of Li^+ vacancies in these compounds. The introduction of Li^+ vacancies has been related to an increase in aliovalent metal substitution level and also correlates to reaction temperature and time.[3] Importantly, Rietveld refinement against PND data was able to confirm the presence of Li(2) vacancies (y) in the majority of samples prepared using microwaves (Table 2). Negligible Li(2) vacancies were detected however in the nitridonickelate with the lowest metal content, $x \sim 0.07$ (**1**); refining the Li(2) occupancy caused the refinement to diverge. This was also the case for the copper-containing sample $Li_{2.95}Cu_{0.05}N$ (**7**). As x increased, however, an increase in y values was observed. Hence, for example, for $Li_{3-x-y}Ni_xN$, where $x \sim 0.22$ (**2**) and $x \sim 0.27$ (**3**), y values of 0.24(4) and 0.36(4) were obtained, leading to compounds of stoichiometry $Li_{2.54}Ni_{0.22}N$ and $Li_{2.36}Ni_{0.27}N$, respectively. Although the level of vacancies found in **2** and **3** (*ca.* 10%) was considerably lower than that observed in some other Li_3N-type nitridonickelates (typically ≥30% for $x \sim 0.8$),[2] the y values are commensurate with the lower transition metal content in **1–3**.

Similarly, for the lithium cobalt nitrides (**4–6**) a dependence of y on x was evident; the (unconstrained) refined Li(2) occupancy decreased as the Co occupancy at the Li(1) site increased. For example, for $x = 0.1$, there are approximately 3% vacancies at the Li(2) site, which then increases to 20% when the amount of metal substituted increases to $x = 0.21$. Accordingly, the PND data indicate stoichiometries of $Li_{2.84}Co_{0.10}N$ (**4**), $Li_{2.45}Co_{0.17}N$ (**5**) and $Li_{2.41}Co_{0.21}N$ (**6**) for our lithium cobalt nitride compounds. Although the cobalt contents are lower here, the vacancy levels of **5** and **6** are in line with those reported by Takeda *et al.* from electrochemical Li extraction of $Li_{2.6}Co_{0.4}N$ (*ca.* 15%)[16] and also by Gordon *et al.*, who identified Li(2) vacancy levels above 20% for $Li_{3-x-y}Co_xN$ with $0.53 \leq x \leq 0.6$.[17]

Assuming oxidation states of +1 and −3 for Li and N respectively, nominal transition metal oxidation states of +1 (**1**), +2.1 (**2**), and +2.4 (**3**); and +1.6 (**4**), +3.2 (**5**), +2.8 (**6**) and +1 (**7**) could be assigned. Given the elevated levels of vacancies in samples of higher x (such as **5** and **6**) and previously reported correlations between y and reaction temperature, one might deduce that the temperatures achieved in these relatively low power MW reactions are in excess of 873 K. Hence as a result and as for similar nitrides prepared by conventional heating,[2,15] in most cases transition metal substitution is essentially aliovalent. The presence of higher oxidation states for the metals in **5** and **6** might be rationalised in terms of the redox chemistry of Co.

Indeed, during electrochemical lithium extraction of $Li_{2.6}Co_{0.4}N$, the nominal Co oxidation reaches a maximum value of *ca.* +5, assuming that only cobalt oxidation charge-compensates for the loss of 1.6 Li ions. In fact, given the unrealistic oxidation state for cobalt in the delithiated compounds, a mechanism for charge balance involving also nitrogen oxidation has been proposed previously. Such a hypothesis is supported experimentally by electron energy-loss spectroscopy (EELS) in $Li_{2.6}Co_{0.4}N$; both cobalt and nitrogen are apparently oxidised when vacancies form during Li extraction.[18]

An alternative charge compensating mechanism might invoke the presence of hydrogen (as $H^{\delta+}$) bonded to nitrogen (creating partial imide substitution), although there is no experimental evidence to corroborate this for **1–6**, (*e.g.* typical N–H bands from the NH^{2-} group were not observed in either the Raman or IR spectra of the as-formed materials). Imide substitution (N–H bond formation) has been previously suggested as one means by which the necessary defect structure is created to enable fast lithium ion conductivity in Li_3N itself. The presence of naturally abundant hydrogen at implied concentrations approaching 20% could not be detected in our PND measurements either from negative peaks in difference Fourier maps (given its scattering length of $b = -3.75$ fm) or from an increased background (arising from its large incoherent scattering cross section).[19]

The MW syntheses described in this work are possible due to the ability of the starting materials (Li_3N and metal powders) to absorb microwave energy and convert this to heat. As electrical conductors, the finely divided metal powder starting materials provide heat (*i.e. via* Ohmic heating) to the reaction mixture[20–22] and the inherent ionic conductivity[23] and semiconducting behaviour[24] of Li_3N would be expected to produce heat *via* mixed conduction mechanisms in a

 This journal is © the Partner Organisations 2015

Open Access Article. Published on 23 September 2015. Downloaded on 2/11/2026 11:55:22 AM.
This article is licensed under a Creative Commons Attribution 3.0 Unported Licence.

microwave field.[25] In fact, it is well established that microwaves couple directly to charge carriers, accelerating the reactions in which good ionic conductors and semiconductors are employed.[26] The ability of other semiconductors such as SiC to generate heat due to matter-radiation interaction has been exploited for example, in use as microwave susceptors (*e.g.* PHEs (passive heating elements)).[27] Furthermore, the outstanding microwave susceptibility of ionic liquids, for example, is attributed to their high ionic conductivity (and polarizability).[28,29] The properties of the metal and nitride starting materials are thus important in being able to design a microwave reaction without an external susceptor (such as carbon, typically) and thus minimise possible contamination of products.

Following a few seconds of irradiation, a purple plasma was observed near the reagents (Fig. 2b). Characteristic purple nitrogen plasmas induced by arc discharge were also observed at 10^{-2} Pa by Aoki *et al.* and other coloured plasmas are common during microwave processing under gaseous environments (*e.g.* sulfur produces a blue plasma).[30,31] We attribute the onset of this plasma formation to an increase in temperature and a variation in the N_2 partial pressure inside the nitrogen-filled reaction vessel caused by the decomposition of Li_3N, which occurs at ~800 °C ($\Delta H = -171.3$ kJ mol^{-1}) (eqn (1)):[32,33]

$$2Li_3N_{(s)} \rightarrow 6Li_{(g)} + N_{2(g)} \quad (1)$$

In our experiments N_2 plasmas were more prevalent (and of longer duration) when reactions were performed in a gaseous nitrogen atmosphere. In fact, it was observed that when the reactions were conducted in an argon atmosphere, longer reaction times were required (**6**). This suggests that plasma formation (and Li_3N decomposition) probably play a key role in the reaction proceeding. The purple N_2 plasma was followed on most occasions by yellow/orange flashes (ESI; Fig. S1†) that were related to Li evaporation, which occurs at *ca.* 1300 °C.[34] Similar observations were made in the previous work by Houmes and zur Loye[4] and in the case of reactions to form $Li_{3-x-y}MN$ from Li_3N and M, Li is an expected byproduct. The ability to maintain homogeneity and phase purity of products in our reactions depends upon the use of the well-defined electric field distribution from the single mode cavity reactor and the ability to limit reaction temperature (and gradients) through a lower applied power than is typical with a multimode cavity (MMC) dometic microwave oven.

Under the specific conditions employed in our synthesis experiments, the maximum metal loading of the MW-ternary compounds was found to be lower (x = 0.27 (**3**), x = 0.21 (**6**) and x < 0.1 (**7**), for M = Ni, Co and Cu respectively) than some of those in the $Li_{3-x-y}M_xN$ compounds previously reported in the literature.[3,15,17] Difficulties in achieving higher transition metal doped samples might be rationalised in terms of the high electric conductivity of the metals. Within the electric field of the MW, the finely divided metal powders are anticipated to generate significant heat (Co powders can achieve 700 °C after 3 minutes of MW exposure using a MMC at 1 kW).[35] Li_3N and transition metal susbstituted derivatives typically decompose at *ca.* 750 °C and so increasing the metal content in the reactant mixtures might be expected to yield reaction temperatures in excess of this decomposition limit, leading to further evaporation of lithium. Accordingly, this might contribute to the lower substitution limits obtained in these MW reactions when using copper, which has an electrical conductivity *ca.* four times higher than Ni or Co [5.96×10^7 S m^{-1} (20 °C)].[36] Higher substitution levels might be achieved by adding additional Li_3N to initial products, regrinding and reheating, but a more satisfactory alternative would be to modify the design of the cavity and/or utilise alternative reactants that do not couple as strongly to the microwave field.

The electrochemical behaviour of these as-synthesised nitridometallate samples was studied *via* galvanostatic measurements (see ESI; Fig. S2–S5†). The nickel–nitride sample with the highest level of Li vacancies determined by PND (**3**) reached a discharge capacity of 458 mA h g^{-1}. This capacity however, was reduced to 175 mA h g^{-1} by the 5th cycle (Fig. S3†). Similarly, the cobalt–nitride sample (**5**) showed a capacity of 642 mA h g^{-1} that faded to 95 mA h g^{-1} after the 5th cycle (Fig. S5†). This capacity fade was irreversible and noted up to 50 cycles for both compounds. The insertion of Li^+ in both materials is most likely made possible by the presence of cation vacancies in the $Li_{3-x}M_xN$ structure and confirms our results obtained from neutron data and the previous reports in the literature.[2] The charging curves during the first cycle for samples **3** and **5** show two well defined segments as previously observed in the literature;[16,18,37,38] first, the voltage gradually increases until *ca.* 1.2 V ($x \sim 0.3$ Li deintercalated) (**3**) and 1.1 V ($x \sim 0.3$ Li deintercalated) (**5**) and then plateaux at the above mentioned potentials followed. These data show that this process clearly affects the following charge–discharge cycles, which in turn, correspond to single-phase mechanisms. Nevertheless, the formation of these plateaux during the first charging process accounts for the initial high capacity in these materials. These features are quite representative of these type of materials and hence agree with previous reports in the literature.[16,18,37,38] Further electrochemical tests to optimise the processing of the electrode are underway.

Conclusions

$Li_{3-x-y}M_xN$ (M = Co, Ni and Cu) materials, which find potential applications in lithium ion batteries, have been synthesised in a single mode cavity MW reactor on unprecedented timescales, orders of magnitude faster than previously documented. PXD and ToF PND data demonstrated that these syntheses can yield single phase materials without the need for a microwave susceptor. Diffraction data also confirmed that the nitridometallates resemble those prepared by conventional heating in terms of their stoichiometry and defect structure. Li^+ ion vacancies are created *via* the aliovalent substitution of M^{n+} ($n > 1$) for Li^+. These experiments demonstrate both that complex nitrides and lithium-containing electrode materials can be synthesised as phase-pure

Open Access Article. Published on 23 September 2015. Downloaded on 2/11/2026 11:55:22 AM.
This article is licensed under a Creative Commons Attribution 3.0 Unported Licence.

compounds by energy-efficient methods; appropriate reactor and experiment design are key factors. Furthermore, we have corroborated by means of electrochemical insertion that Li^+ vacancies were present and that these materials can (de)intercalate lithium in the voltage range 0–1.4 V at C/30 rate with initial discharge capacities of 458 mA h g^{-1} and 642 mA h g^{-1} for the samples with higher metal doping levels (and Li-vacancies); *i.e.* $Li_{2.36}Ni_{0.27}N$ and $Li_{2.41}Co_{0.21}N$. It should thus be possible to extend the methodology to the sustainable synthesis and processing of a wide range of other important battery materials.

Acknowledgements

DHG thanks ScotCHEM for a SPIRIT (Scottish Funding Council) PhD studentship for NTR (ref. HR08001) and STFC for provision of neutron beam time at ISIS. SAC gratefully acknowledges funding support from the EPSRC (EP/K029290/1) and the allocation of a PhD scholarship from the University of Glasgow.

Notes and references

1 (*a*) T. Shodai, S. Okada, S. Tobishima and J. Yamaki, *J. Power Sources*, 1997, **68**, 515; (*b*) Y. Takeda, M. Nishijima, M. Yamahata, K. Takeda, N. Imanishi and O. Yamamoto, *Solid State Ionics*, 2000, **130**, 61.
2 D. H. Gregory, P. M. O' Meara, A. G. Gordon, J. P. Hodges, S. Short and J. D. Jorgensen, *Chem. Mater.*, 2002, **14**, 2063.
3 Z. Stoeva, R. I. Smith and D. H. Gregory, *Chem. Mater.*, 2006, **18**, 313.
4 J. D. Houmes and H.-C. zur Loye, *J. Solid State Chem.*, 1997, **130**, 266.
5 A. J. Anderson, R. G. Blair, S. M. Hick and R. B. Kaner, *J. Mater. Chem.*, 2006, **16**, 1318.
6 A. Rabenau and H. Schulz, *J. Less-Common Met.*, 1976, **50**, 155.
7 G. Nolze and W. Kraus, *Powder Diffr.*, 1998, **13**, 256.
8 J. Laugier and B. Bochu, Laboratoire des Materiaux et du Génie Physique de L'Ecole Supérieure de Physique de Grenoble; http://www.inpg.fr/LMGP, accessed on 28/04/13.
9 A. C. Larson and R. B. Von Dreele, *The General Structure Analysis System*, Los Alamos National Laboratories, Los Alamos, NM, 2000.
10 B. H. Toby, *J. Appl. Crystallogr.*, 2001, **34**, 210.
11 W. Sachsze and R. Juza, *Z. Anorg. Chem.*, 1949, **259**, 278.
12 R. Niewa, Z.-L. Huang, W. Schnelle, Z. Hu and R. Kniep, *Z. Anorg. Allg. Chem.*, 2003, **629**, 1778.
13 Z. Stoeva, R. Gomez, D. H. Gregory, G. B. Hix and J. J. Titman, *Dalton Trans.*, 2004, 3093.
14 A. G. Gordon, D. H. Gregory, A. J. Blake, D. P. Weston and M. O. Jones, *Int. J. Inorg. Mater.*, 2001, **3**, 973.
15 M. G. Barker, A. J. Blake, D. H. Gregory, D. J. Siddons, S. E. Smith, P. P. Edwards and T. A. Hamor, *Chem. Commun.*, 1999, 1187.
16 Y. Takeda, M. Nishijima, M. Yamahata, K. Takeda, N. Imanishi and O. Yamamoto, *Solid State Ionics*, 1996, **86**, 785.
17 A. G. Gordon, R. I. Smith, C. Wilson, Z. Stoeva and D. H. Gregory, *Chem. Commun.*, 2004, 2812.
18 S. Suzuki, T. Shodai and J. Yamaki, *J. Phys. Chem. Solids*, 1998, **59**, 331.
19 V. F. Sears, *Neutron News*, 1992, 3, 26.
20 A. G. Whittaker and D. M. Mingos, *J. Chem. Soc., Dalton Trans.*, 1995, 2073.
21 R. Roy, D. Agrawal, J. Cheng and S. Gedevanishvili, *Nature*, 1999, **399**, 668.
22 H. J. Kitchen, S. R. Vallance, J. L. Kennedy, N. Tapia-Ruiz, L. Carassiti, A. Harrison, A. G. Whittaker, T. D. Drysdale, S. W. Kingman and D. H. Gregory, *Chem. Rev.*, 2014, **114**, 1170.
23 B. A. Boukamp and R. A. Huggins, *Mater. Res. Bull.*, 1978, **13**, 23.
24 D. H. Gregory, *J. Mater. Chem.*, 2008, **18**, 2321.
25 N. Tapia-Ruiz, N. Sorbie, N. Vaché, T. K. A. Hoang and D. H. Gregory, *Materials*, 2013, **6**, 5410.
26 A. Harrison, R. Ibberson, G. Robb, G. Whittaker, C. Wilson and D. Youngson, *Faraday Discuss.*, 2002, **122**, 363.
27 J. M. Kremsner and C. O. Kappe, *J. Org. Chem.*, 2006, **71**, 4651.
28 S. Mallakpour and A. Zadehnazari, *Adv. Polym. Technol.*, 2013, **32**, 21333.
29 T. E. Ashton, J. Vidal Laveda, D. A. MacLaren, P. J. Baker, A. Porch, M. O. Jones and S. A. Corr, *J. Mater. Chem. A*, 2014, **2**, 6238.
30 R. Kniep, *Angew. Chem., Int. Ed.*, 1993, **32**, 1411.
31 H. Aoki, K. Takahashi, K. Takaki and T. Fujiwara, *IEEE T. Plasma Sci.*, 2011, **39**, 2912.
32 P. F. Adams, P. Hubberstey and R. J. Pulham, *J. Less-Common Met.*, 1975, **42**, 1.
33 H. Kimura, M. Asano and K. Kubo, *J. Nucl. Mater.*, 1980, **91**, 200.
34 R. C. Weast and M. J. Astle, *Handbook of Chemistry and Physics*, CRC Press, Inc, 61st edn, 1980.
35 K. J. Rao, B. Vaidhyananathan, M. Ganguli and P. A. Ramakrishnan, *Chem. Mater.*, 1999, **11**, 882.
36 D. Griffiths, *Introduction to Electrodynamics*, Prentice Hall, Upper Saddle River, New Jersey, 3rd edn, 1999, p. 286, ISBN 0-13-805326.
37 M. Nishijima, T. Kagohashi, Y. Takeda, M. Imanishi and O. Yamamoto, *J. Power Sources*, 1997, **68**, 510.
38 T. Y. Kim, M. G. Kim, J. M. Lee, T. Kang and H.-J. Sohn, *Electrochem. Solid-State Lett.*, 2002, **5**, A103.

 This journal is © the Partner Organisations 2015